Molecular Psychiatry (2014) 19, 129–139

www.nature.com/mp

ORIGINAL ARTICLE

Functional genetic variants in the vesicular monoamine transporter 1 modulate emotion processing

FW Lohoff[1], R Hodge[1], S Narasimhan[1], A Nall[1], TN Ferraro[1], BJ Mickey[2], MM Heitzeg[2], SA Langenecker[2], J-K Zubieta[2], R Bogdan[3,4], YS Nikolova[3], E Drabant[5], AR Hariri[3], L Bevilacqua[6], D Goldman[6] and GA Doyle[1]

Emotional behavior is in part heritable and often disrupted in psychopathology. Identification of specific genetic variants that drive this heritability may provide important new insight into molecular and neurobiological mechanisms involved in emotionality. Our results demonstrate that the presynaptic vesicular monoamine transporter 1 (*VMAT1*) Thr136Ile (rs1390938) polymorphism is functional *in vitro*, with the Ile allele leading to increased monoamine transport into presynaptic vesicles. Moreover, we show that the Thr136Ile variant predicts differential responses in emotional brain circuits consistent with its effects *in vitro*. Lastly, deep sequencing of bipolar disorder (BPD) patients and controls identified several rare novel *VMAT1* variants. The variant Phe84Ser was only present in individuals with BPD and leads to marked increase monoamine transport *in vitro*. Taken together, our data show that *VMAT1* polymorphisms influence monoamine signaling, the functional response of emotional brain circuits and risk for psychopathology.

Molecular Psychiatry (2014) **19,** 129–139; doi:10.1038/mp.2012.193; published online 22 January 2013

Keywords: amygdala; bipolar disorder; medial PFC; schizophrenia; SLC18A1

INTRODUCTION

Effective regulation of our emotional responses is critical for normal human behavior and often disrupted in psychopathology. Although key brain regions and circuits, such as the prefrontal cortex (PFC), anterior cingulate cortex (ACC) and the amygdala,[1] have been identified that underlie affective processing, little is known about the underlying molecular mechanisms that contribute to individual differences in the functioning of these circuits. The observed variance in emotional behavior is partly heritable with approximately half of the interindividual variability attributed to genetic variation.[2,3] Identification of specific genetic variants, which drive this heritability, may provide important new insight into molecular and neurobiological mechanisms that shape individual differences in emotional behavior and risk for psychopathology.

Previous research has shown that genetic variation in plasma membrane transporters, such as the serotonin (5-HT), norepinephrine (NE) and dopamine (DA) transporters, influence interindividual responses in brain circuits supporting emotional behavior.[3] These transporters are primarily involved in synaptic neurotransmitter *reuptake*, which contributes to the *duration* of signaling, but could be considered largely 'after the fact'. In contrast, variation in the *magnitude* of signaling may be more closely related to mechanisms regulating synaptic neurotransmitter *release*. Despite its importance, the effect of variability in presynaptic monoamine packaging and release on individual differences in human emotional behavior is poorly understood.

Vesicular monoamine transporters (VMATs) package neurotransmitter molecules into presynaptic storage vesicles that release their contents into the synaptic cleft upon arrival of an action potential at the nerve terminal. Two structurally related but pharmacologically distinct VMATs have been identified, encoded by separate genes, *VMAT1* (*SLC18A1*) located on chromosome 8p21 and *VMAT2* (*SLC18A2*) located on chromosome 10q25.[4–6] Although it was thought initially that only VMAT2 is expressed in the brain,[6,7] expression of *VMAT1* in mouse, rat and human brain has been shown recently.[8–10] Both genes are differentially expressed in the brain during embryonic development.[10] In structure, VMATs are similar in size and molecular topography to other plasma membrane transporters, such as the DA transporter, 5-HT transporter and NE transporter, with 12 transmembrane domains and both tails located in the interior.[4] Nevertheless, VMAT physiology is distinct from plasma membrane transporters in that they use a proton gradient to transport substrates and lack an extracellular compartment. Both proteins are able to transport monoamines; however, they differ in their substrate preferences and affinities. *VMAT1* has higher affinity for serotonin,[11] whereas *VMAT2* is also able to transport histamine.[6]

Interestingly, no data exist on presynaptic monoaminergic vesicle transport and effects on emotion processing in human; however, indirect evidence suggests that alteration in presynaptic loading of vesicle with catecholamines has an effect on mood states and emotional behavior. For example, reserpine, a non-selective irreversible VMAT inhibitor, which causes monoamine depletion and 'depressive-like' phenotypes in rodents, was introduced in 1954 as an antipsychotic and antihypertensive medication, and was instrumental in the development of the 'monoamine hypothesis' of affective disorders.[12] However, clinical

[1]Translational Research Laboratories, Department of Psychiatry, Center for Neurobiology and Behavior, University of Pennsylvania School of Medicine, Philadelphia, PA, USA; [2]Department of Psychiatry, Molecular and Behavioral Neuroscience Institute, University of Michigan, Ann Arbor, MI, USA; [3]Department of Psychology and Neuroscience, Institute for Genome Sciences and Policy, Duke University, Durham, NC, USA; [4]Department of Psychology, Washington University in St Louis, St Louis, MO, USA; [5]23andMe, Mountain View, CA, USA and [6]Laboratory of Neurogenetics, National Institute on Alcohol Abuse and Alcoholism, Rockville, MD, USA. Correspondence: Dr FW Lohoff, Translational Research Laboratories, Department of Psychiatry, Center for Neurobiology and Behavior, University of Pennsylvania School of Medicine, 125 South 31st Street, Room 2213, Philadelphia, PA 19104, USA.
E-mail: lohoff@mail.med.upenn.edu
Received 23 July 2012; revised 12 November 2012; accepted 16 November 2012; published online 22 January 2013

use of reserpine has been limited owing to many drug interactions and side effects, which include lethargy and clinical depression.[13–15] Consistent with the effects of reserpine, mice lacking *VMAT2* die within a few days of birth and heterozygotes for the gene knockout have decreased monoamine levels and increased sensitivity to monoamine neurotoxicity as well as depressive-like phenotypes.[16–22] Therefore, genetic variation in *VMAT1* and/or *VMAT2* may contribute to differences in vesicular transport and vesicle filling, which may in turn affect monoaminergic signaling in emotional brain circuits and, subsequently, emotional behavior and risk for psychopathology.

In this paper, we focus on *VMAT1*, which has recently emerged as a candidate gene for neuropsychiatric disorders. Several reports have shown that common missense variants in *VMAT1* are associated with bipolar disorder (BPD), schizophrenia (SZ), anxiety-related personality traits and cognitive phenotypes related to SZ.[23–29] This is remarkable since the *VMAT1* gene is located on chromosome 8p, a region previously implicated as a shared genomic susceptibility region for SZ/BPD in linkage scans. The fact that several common missense variations in this gene have been associated with different psychiatric phenotypes suggests that certain fundamental neurobiological mechanisms are shared between psychiatric phenotypes, leading to pleiotropy. This observation has been made for multiple other candidate genes[30] and supports the hypothesis that our current nosology is not reflecting underlying neurobiology.[31,32]

Here, we used a translational research approach to investigate the neural mechanism underlying emotional behavior modulated by variation in the presynaptic *VMAT1* gene using a step-wise approach beginning with identification of a functional locus, namely a common missense variant, and tracing effects of this variant on behavior via two functional magnetic resonance imaging (fMRI) paradigms in independent samples. We find that Thr136Ile (rs1390938) is functional *in vitro*, with the Ile allele leading to increased monoamine transport into presynaptic vesicles. Thr136Ile is shown to cause altered metabolic responses to emotional probes in brain regions implicated in emotional behavior. Furthermore, to assess the potential contribution of rare variation, deep sequencing of BPD patients and controls identified several rare novel *VMAT1* variants. A variant Phe84Ser that was exclusively present in individuals with BPD also leads to a marked increase in monoamine transport *in vitro*.

MATERIALS AND METHODS

In vitro assays

Plasmid construction and mutagenesis. The coding sequence of the human *VMAT1* gene (*SLC18A1*) was amplified from commercially available cDNA extracted from post-mortem human substantia nigra tissue (Clontech, Mountain View, CA, USA) (Figure 1b). ExPand High Fidelity Polymerase (Roche, Indianapolis, IN, USA) and 1 M betaine were used in the polymerase chain reaction (PCR) cocktail with forward (5′-CCTCCCCTCTTCCA-3′) and reverse (5′-GATTCCCAGGCAGA-3′) primers. The thermocycling protocol was as follows: 94 °C for 5 min, followed by 40 cycles of 94 °C for 1 min, 60 °C for 1 min and 72 °C for 2 min. The final extension was 72 °C for 5 min. PCR product was directly T/A cloned into the vector (TOPO TA Cloning Kit; Invitrogen, Grand Island, NY, USA). *SLC18A1* cDNA was released from the pCRII-TOPO vector by *Xho*I and *Bam*HI digest. *Bam*HI-*VMAT1*-*Xho*I cDNAs were then ligated into pcDNA5/FRT that had been digested with *Bam*HI and *Xho*I.

Sanger sequencing revealed our initial clone contained *SLC18A1* cDNA encoding the VMAT1 protein isoform with threonines at amino-acid positions 4, 98 and 136 (Thr–Thr–Thr isoform).

Site-directed mutagenesis (QuikChange; Stratagene, Santa Clara, CA, USA) was used to create VMAT1 isoforms with common haplotypes and rare variants (Supplementary Table 4). The thermocycling protocol for all site-directed mutagenesis reactions was as follows: 95 °C for 30 s, followed by 12 cycles of 95 °C for 30 s, 60 °C for 1 min and 68 °C for 8 min. The final extension was 68 °C for 7 min. Mutated *SLC18A1* plasmid amplicons were treated with *Dpn*I, transformed into competent XL1-Blue *Escherichia coli* and the plasmid DNA of various clones prepared and *VMAT1* fully sequenced by Sanger sequencing to ensure the absence of unwanted mutations before being used in subsequent *in vitro* analyses.

Transfections. Empty pcDNA5/FRT vector or pcDNA5/FRT-*VMAT1* constructs were cotransfected with pOG44 into Flp-in CV-1 (Invitrogen) cells using Lipofectamine 2000 and Plus reagent (Invitrogen), according to the manufacturer's recommendations. Stable *VMAT1*-expressing clones (Pro4–Thr98–Thr136, Thr4–Ser98–Thr136, Thr4–Thr98–Thr136 or Thr4–Thr98–Ile136) were selected by the addition of hygromycin to the growth medium and clonal colonies were then isolated and expanded for further analysis. For transient transfections, Flp-in CV-1 cells (4×10^4) were transfected with 0.5 μg human *VMAT1* construct, pcDNA5/FRT or no DNA (mock) using the TransIT-LT1 Transfection Reagent (Mirus Corp., Madison, WI, USA).

hVMAT1 expression analysis (immunoblots). Flp-in CV-1 cells stably transfected with human *VMAT1* constructs Pro4–Thr98–Thr136, Thr4–Ser98–Thr136 or Thr4–Thr98–Ile136 (Figure 1b) were washed two times with 1 ml phosphate-buffered saline (PBS) and 0.25 ml trypsin, and 0.05% ethylenediaminetetraacetic acid was added to disassociate cells from the plate. Trypsinization was stopped with the addition of 0.5 ml Dulbecco's modified Eagle's medium (completed with 10% fetal bovine serum and 0.1% PenStrep). Cells were centrifuged at 500 *g* for 5 min at 4 °C, medium was removed and pellets were washed three times with PBS. After washing, cells were lysed on ice in 300 μl Triton X-100 lysis buffer for 15 min on ice and centrifuged at 2500 *g* for 10 min at 4 °C to remove nuclei and cellular debris. Total soluble protein was quantified using the BCA Protein Assay (Pierce; Rockford, IL, USA) and a Bio-Tek Instruments μQuant Spectrophotometer (Winooski, VT, USA). To determine *VMAT1* expression levels from stable cell lines, 50 μg of isolated protein was heated at 70 °C for 10 min in the presence of 1 × NuPAGE LDS Sample Buffer and Sample Reducing Agent (Invitrogen). Prestained sodium dodecyl sulfate-polyacrylamide gel electrophoresis broad range standards (Bio-Rad, Hercules, CA, USA) were used as a sizing ladder. Proteins were separated by electrophoresis at 200 V for 50 min on a NuPAGE Novex 10% Bis-Tris gel in 1 × NuPAGE MOPS SDS Running Buffer and Antioxidant (Invitrogen), electrophoretically transferred to a nitrocellulose membrane at 30 V for 90 min in 1 × NuPAGE Transfer Buffer and Antioxidant (Invitrogen). Membranes were blocked for 2 h in 10% non-fat dry milk. Blocked membranes were immunoblotted with primary antibody SC-7718 (Santa Cruz Biotechnology, Santa Cruz, CA, USA) at a dilution of 1:300 for 48 h. Blots were then washed once with 200 ml 1 × Tris-buffered saline with 0.1% Tween-20 (TBS-T) for 15 min and three times with 50 ml 1 × TBS-T. Bound primary antibody was detected by incubation for 1 h with a horseradish peroxidase-conjugated anti-goat secondary antibody at a 1:10 000 dilution. Chemiluminescence was generated by incubating membranes with an ECL Plus Western Blotting Detection Kit (Amersham Biosciences, Piscataway Township, NJ, USA) and blots were then exposed to HyBlot CL film (Denville Scientific, South Plainfield, NJ, USA) for various times. (Figure 1b) Primary and secondary antibodies were stripped from the membranes using Restore™ Western Blot Stripping Buffer (Pierce), washed two times in 50 ml 1 × TBS-T for 5 min and membranes were again blocked overnight in 10% non-fat dry milk. Blocked membranes were probed for β-actin with primary antibody MAB 1501 (Millipore, Billerica, MA, USA) at a dilution of 1:1000 for 1 h. Blots were then washed once with 200 ml 1 × TBS-T for 15 min and three times with 50 ml 1 × TBS-T. Bound primary antibody was detected by incubation for 30 min with a horseradish peroxidase-conjugated anti-mouse secondary antibody at a 1:10 000 dilution. Chemiluminescence was generated and blots exposed to film as described above.

To determine VMAT1 expression levels in Flp-in CV-1 cells transiently transfected with human *VMAT1* constructs used in the uptake assays, 3 μg of total protein isolated from transfected cells were heated at 70 °C for 10 min in the presence of 1 × NuPAGE LDS Sample Buffer and Sample Reducing Agent (Invitrogen). Prestained Novex Sharp Protein standards (Invitrogen) were used as a sizing ladder. Proteins were separated by electrophoresis at 200 V for 1 h on a NuPAGE Novex 4–12% Bis-Tris gel in 1 × NuPAGE MOPS SDS Running Buffer and Antioxidant (Invitrogen), electrophoretically transferred to a nitrocellulose membrane using Invitrogen's iBlot Dry Blotting System. Membranes were blocked overnight in 10% non-fat dry milk. Blocked membranes were immunoblotted with primary antibody SC-7718 (Santa Cruz Biotechnology) at a dilution of 1:500 for 48 h. Blots were then washed once with 200 ml 1 × TBS-T for 15 min and three times with 50 ml 1 × TBS-T. Bound primary antibody was

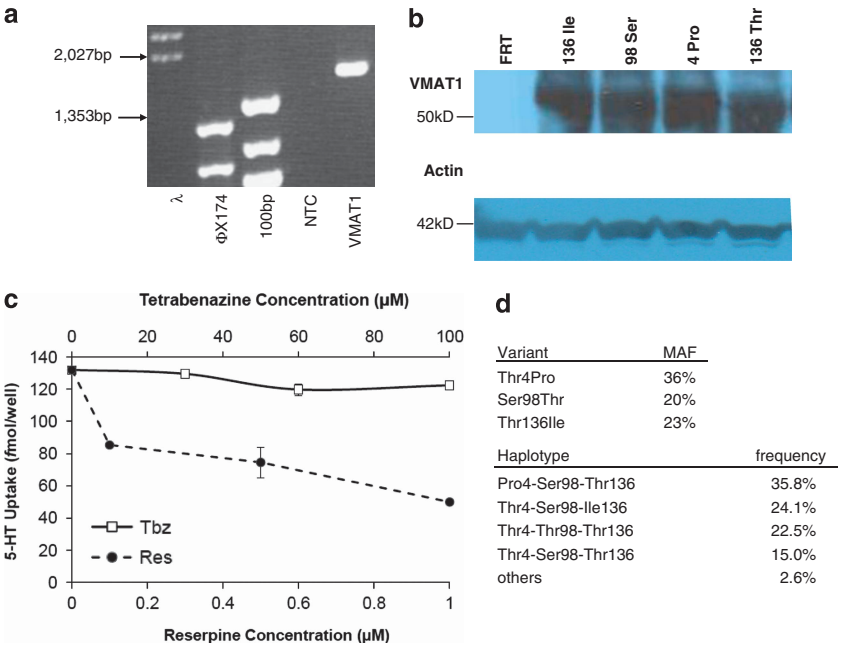

Figure 1. Common human vesicular monoamine transporter 1 (*VMAT1*) variants and haplotypes used for transfection of CV-1 cell lines. (**a**) *VMAT1* is expressed in human brain: full-length VMAT1 cDNA amplified from human substantia nigra (*VMAT1*). NTC, no-template control; 100 bp, NEB 100 bp ladder; ΦX174, ΦX174 DNA/*Hae*III digest marker; λ, bacteriophage λ DNA-*Hind*III digest marker. (**b**) Transfected CV-1 cell lines express VMAT1 protein: immunoblot showing expression of human *VMAT1* variants (136Ile, 98Ser, 4Pro and 136Thr) in VMAT1 stable transfected, but not control (FRT; empty vector transfected) CV-1 cells. β-Actin is shown as a loading control. (**c**) Pharmacological characterization showing serotonin (5-HT) uptake by VMAT1 construct is inhibited by reserpine (RES; VMAT1 and VMAT2 inhibitor) but not tetrabenazine (TBZ; VMAT2-only inhibitor). Uptake of [^{3}H]5-HT in digitonin-permeabilized CV-1 cells expressing Thr–Thr–Ile isoform of VMAT1 in the presence of RES and TZB. Top x axis reflects concentration of TZB (μM), while bottom x axis reflects RES concentration (μM). [H]5-HT uptake values presented are blanked against uptake by CV-1 cells transfected with empty pcDNA5/FRT vector. (**d**) Common VMAT1 single-nuleotide polymorphisms (SNPs) and the haplotypes they form, and minor allele frequencies are shown for European Americans.

detected by incubation for 1 h with a horseradish peroxidase-conjugated anti-goat secondary antibody at a 1:10 000 dilution. Chemiluminescence was generated and blots exposed to film as described above. Primary and secondary antibodies were stripped from the membranes using ReBlot Plus Strong Antibody Stripping Solution (Millipore), washed two times in 50 ml 1 × TBS-T for 5 min and membranes were again blocked overnight in 10% non-fat dry milk. Blocked membranes were probed for β-actin with primary antibody MAB 1501 (Millipore) at a dilution of 1:1000 for 1 h. Blots were then washed once with 200 ml 1 × TBS-T for 15 min and three times with 50 ml 1 × TBS-T. Bound primary antibody was detected by incubation for 30 min with a horseradish peroxidase-conjugated anti-mouse secondary antibody at a 1:10 000 dilution. Chemiluminescence was generated and blots exposed to the film as described above.

Pharmacological analysis. Flp-in CV-1 cells stably expressing the Thr–Thr–Ile *VMAT1* isoform were used to verify the pharmacological characteristics of the protein. [^{3}H]5-HT was used in a modified monoamine uptake assay. The [^{3}H]monoamine uptake protocol (see below) was modified such that before addition of the [3H]5-HT, digitonin-permeabilized cells were preincubated with reserpine or tetrabenazine at various concentrations in uptake buffer (Figure 1c).

[^{3}H]monoamine uptake. Monoamine uptake was performed with a protocol similar to those used in previous studies.[33,34] For the analysis of common haplotypes and rare variants, Flp-in CV-1 cells were plated in 24-well Bio-Coat Type I Collagen plates (BD Biosciences, San Jose, CA, USA). Cells (4×10^4) were transiently transfected with 0.5 μg human *VMAT1* constructs using the TransIT-LT1 Transfection Reagent (Mirus Corp.). After 48 h, cells were washed with 1 ml PBS at room temperature containing magnesium chloride and calcium chloride, and then incubated in 1 ml uptake buffer (110 mM potassium tartrate, 5 mM glucose, 0.2% bovine serum albumin, 200 μM calcium chloride, 1 mM ascorbic acid, 1 μM pargyline, 25 mM HEPES) for 5 min at room temperature. Cells were then incubated in uptake buffer with 10 μM digitionin at 37 °C for 10 min, followed by a 10-min incubation in 0.5 ml uptake buffer containing 5 mM MgATP and ~0.1 μM ^{3}H-labeled monoamine. Cells were then placed on ice and washed once with 1 ml ice-cold uptake buffer for 1 min and two times with ice-cold 1 ml PBS containing magnesium chloride and calcium chloride for 1 min. After washing, cells were solubilized in 0.5 ml 1% sodium dodecyl sulfate at room temperature, transferred to scintillation vials and 10 ml Eco-Lite Scintillation Fluid was added. Samples were shaken and incubated in the dark for 30 min before counting with a Wallac 1209 Rackbeta Liquid Scintillation Counter (Perkin Elmer, Waltham, MA, USA). Counts per minute were recorded for each sample and used to calculate the fmol amount of ^{3}H-labeled monoamine taken up per well. All experiments were carried out at least four times in triplicates.

VMAT1 expression was determined by immunoblotting (see above). Before uptake assay analysis, two wells (duplicates) containing Flp-in CV-1 cells transiently transfected with the same TransIT-LT1:DNA complexes as the uptake assay cells were washed two times with 1 ml PBS and 0.25 ml trypsin 0.05% EDTA was added to disassociate cells from the Bio-Coat Type I Collagen plates. Trypsinization was stopped with the addition of 0.5 ml Dulbecco's modified Eagle's medium (completed with 10% fetal bovine serum and 0.1% PenStrep). Cells were centrifuged at 500 *g* for 5 min at 4 °C, medium was removed and pellets were washed three times with 50 μl PBS. After washing, cells were lysed on ice in 20 μl Igepal CA-630 non-denaturing lysis solution for 15 min and centrifuged at 2500 *g* for 10 min at 4 °C to remove nuclei and cellular debris. Total protein was quantified using the Pierce BCA Protein Assay and a Bio-Tek Instruments μQuant Spectrophotometer. Optical densities for VMAT1 and β-actin proteins detected by immunoblotting (see above) were determined using ImageJ and VMAT1 values were normalized using β-actin values as a loading control. VMAT1 expression normalized to β-actin was then used to normalize ^{3}H-labeled monoamine uptake values determined in parallel in transiently transfected cells (see above). To confirm the result of transient uptake assays for the Thr136Ile variant using the above methods, [^{3}H]monoamine uptake assays using cell lines stably transfected with either Thr4–Thr98–Thr136 or Thr4–Thr98–Ile136 were also carried out (Supplementary Figure. 1). Experiments were repeated at least four times in triplicates.

fMRI emotion word task and *VMAT1* Thr136Ile

The *VMAT1* variant Thr136Ile was genotyped from whole blood using ABI Taqman methodology as described above (rs1390938, major allele G = Thr, minor allele A = Ile).

Subjects. Procedures were approved by the Institutional Review Board at the University of Michigan, and all participants gave written informed consent. Participants were recruited through local advertisement for neuroimaging studies of pain processing and MDD, as described previously.[35,36] Healthy subjects were screened to exclude major medical illness, psychiatric disorder or substance-use disorder. Subjects with MDD were diagnosed with a current moderate-to-severe depressive episode using the Structured Clinical Interview for Diagnostic and Statistical Manual of Mental Disorders, Fourth Edition, administered by an experienced psychiatric research nurse, and diagnosis was confirmed with a clinical interview by a psychiatrist. Comorbid generalized anxiety disorder, social anxiety disorder or specific phobia was permitted, but major medical illness and other Axis I diagnoses were otherwise excluded. All participants were fluent English speakers, and all participants but one were right-handed. All subjects were free of exogenous hormones or medications with central nervous system activity, and they were instructed to abstain from use of all psychoactive substances for 24 h before the study. fMRI data were available from 93 healthy participants and 20 MDD subjects. Of those 113 subjects, 103 provided blood for genotyping (85 healthy and 18 MDD), and genotyping was successful in 102 subjects. In all, 51 (50%) were women, and the mean age was 30 years (s.d. = 10 years, range = 20–58 years). Self-reported race was Caucasian ($n = 72$), African American ($n = 17$), Asian ($n = 5$) or other/mixed ($n = 8$).

Emotion word task. Subjects performed an affective word task during which they silently read emotionally valenced words, as described previously.[35,37] Words were selected from the Affective Norms for English Words list, which provides normative emotional ratings for valence (negative to positive, 1–9) and arousal (low to high, 1–9).[38] We used negative words with valence ratings <3, neutral words with valence ratings between 4.5 and 5.5 and positive words with valence ratings >7. Arousal ratings were >5 for positive and negative words (not significantly different from each other), and >2 for neutral words. Nine participants viewed a list of investigational negative, positive and neutral words that lacked normative ratings, but analyses demonstrated no differences in activation, so they were pooled together. Words were presented on screen for 3 s each, separated by 1 s of fixation, in blocks of six words (E-Prime version 1.1; Psychology Software Tools, Pittsburgh, PA, USA). Participants pressed a button after silently reading each word. With the exception of seven individuals whose behavioral data were corrupted after the experiment, we confirmed that response rates were $>90\%$ for all participants. The block design incorporated 24-s blocks of positive, negative or neutral words separated by 18-s rest periods. Subjects were instructed to rest while viewing crosshairs during the rest periods. Each session included six blocks, counterbalanced by emotional valence using a Latin squares design and each subject completed three runs. Subjects with usable data from at least two runs were included in analyses.

Magnetic resonance imaging. As described previously,[35,36] BOLD signal was measured in the whole brain using a General Electric Signa 3-Tesla scanner (Milwaukee, WI, USA) with a standard radiofrequency coil, using a T2*-weighted pulse sequence (spiral in/out, gradient echo; repetition time (TR) = 2 s; echo time (TE) = 30 ms; flip angle (FA) = 90°; field of view (FOV) = 20 or 24 cm; 64-by-64 image matrix; slice thickness = 3 or 4 mm; 30 oblique–axial slices). A high-resolution T1-weighted scan was also acquired for anatomical localization (three-dimensional spoiled gradient recalled echo; TR = 25 ms; min TE; FOV = 24 cm; 256-by-256 matrix; slice thickness = 1.4 mm). Head motion was minimized by use of foam pads. Data were reconstructed off-line, de-spiked, slice-time corrected, realigned and co-registered. Images from each session were visually inspected for artifacts and screened for excessive head movement (more than 2 mm of translation or 2° of rotation). Functional images were smoothed with a Gaussian kernel (full-width at half-maximum, 6 mm) to reduce residual noise and interindividual variability and resampled at $2 \times 2 \times 2\,mm^3$.

Statistical analysis. BOLD responses were modeled with SPM2 (Wellcome Department of Cognitive Neurology, University College London, UK) using a general linear model and canonical hemodynamic response function, as described previously.[35] Analysis proceeded in two stages. In the first level, activation maps were derived for individual subjects, including task-related covariates of interest and nuisance covariates (head translation and rotation). To allow comparisons across individuals, regressor and contrast images were spatially normalized by warping each subject's T1 image to standard stereotactic space (Montreal Neurological Institute, MNI, Montreal, QC, Canada) using the SPM2 nonlinear algorithm, and applying that transformation to contrast images. In the second level, a random effects analysis was employed to determine average task and group effects. A mask excluded the cerebellum and brainstem below the midbrain because these regions were not well represented. Task effects were determined for two primary contrasts of interest, negative–neutral words and positive–neutral words, which isolated affective processing and controlled for nonspecific lexical and visual processing. As described previously,[35] among 93 healthy participants, the negative–neutral contrast activated a cluster in the medial PFC (peak coordinates = −2, 56, 22; peak $z = 4.3$; cluster size = 2184 mm^3 at one-tailed $P < 0.001$; family-wise error cluster corrected $P = 0.04$). This single task-related ROI was used for hypothesis testing. (No significant activation was found for the positive–neutral contrast.) The average percent signal change in the ROI was computed from regressor images for each subject and analyzed outside of SPM. To test the primary hypothesis that the *VMAT1* Thr136Ile polymorphism affects medial PFC responses to negative words, percent signal change in the ROI was compared between Thr136 homozygotes ($n = 63$) and Ile136 carriers ($n = 39$). Initial power analyses indicated that, with group sizes of 63 and 39, we would have 80–90% power to detect a standardized effect size of 0.3 with a 5% two-tailed type I error rate.[39] Percent signal change was entered as the dependent variable and Ile136 carrier status as the between-subjects factor in a univariate general linear model (PASW Statistics 18.0; SPSS, Chicago, IL, USA). Covariates sex, age, Caucasian race and MDD diagnosis were included in the model as potential confounders. Exploratory analyses were performed after hypothesis testing. To test an additive genetic model, we used linear regression (PASW Statistics 18.0) with the three genotype groups (Ile/Ile, Ile/Thr and Thr/Thr) coded 1, 2 and 3, respectively, controlling for sex, age, Caucasian race and MDD diagnosis. To explore gene effects elsewhere in the brain, we performed a voxel-wise analysis in SPM8 using an analysis of variance model with two groups (Thr136 homozygotes and Ile136 carriers) and with sex, age, Caucasian race and MDD diagnosis as covariates. Spatial coordinates are reported in MNI space.

In contrast to threat-related facial stimuli, this task does not generally engage the amygdala. However, based on observed genetic effects on threat-related amygdala activation, we examined gene effects on amygdala activation in the Emotion Word Task. SPM8 family-wise error correction was applied within a bilateral amygdala mask, defined anatomically based on the Talairach atlas as implemented in the Wake Forest University PickAtlas Toolbox.[40,41]

fMRI amygdala reactivity task and *VMAT1* Thr136Ile

Duke Neurogenetics Study. Genotype (rs1390938 within *SLC18A1*; A/G) and neuroimaging data were available from 298 participants who completed the Duke Neurogenetics Study, an ongoing protocol assessing a wide range of behavioral and biological phenotypes among young adult volunteers. Participants completed an archival challenge paradigm, which robustly elicits threat-related amygdala reactivity.[42] The paradigm consists of four task blocks wherein participants match face stimuli with angry, fearful, surprised or neutral expressions—all of which convey threat-related information—interleaved with five sensorimotor control blocks of matching simple geometric shapes. Regression analyses with gender, self-reported ethnicity and psychopathology as covariates were used to test the association between rs1390938 genotype and threat-related amygdala reactivity.

Participants. All participants ($n = 350$) provided informed consent in accord with the guidelines of the Duke University Medical Center Institutional Review Board, and were in good general health. Study exclusions included: (1) medical diagnoses of cancer, stroke, diabetes requiring insulin treatment, chronic kidney or liver disease, or lifetime history of psychotic symptoms; (2) use of psychotropic, glucocorticoid or hypolipidemic medication; and (3) conditions affecting cerebral blood flow and metabolism (for example, hypertension). Current Diagnostic and Statistical Manual of Mental Disorders, Fourth Edition Axis I and select Axis II disorders (Antisocial Personality Disorder and Borderline Personality Disorder) were assessed with the electronic Mini International

Neuropsychiatric Interview and Structured Clinical Interview for the Diagnostic and Statistical Manual of Mental Disorders, Fourth Edition (SCID) subtests, respectively. These disorders were not exclusionary as the Duke Neurogenetics Study seeks to establish broad variability in multiple behavioral phenotypes related to psychopathology. A total of 52 participants from the initial sample were excluded because of: insufficient DNA yield ($n = 2$), scanner artifacts in fMRI data ($n = 3$), incidental structural brain abnormalities ($n = 3$), a large number of movement outliers in fMRI data ($n = 5$; see ARtifact detection Tool description below), inadequate signal in our amygdala ROIs ($n = 4$) and poor behavioral performance ($n = 35$; accuracy lower than 75%). Thus, all data analyses were conducted in a final sample of 298 (see Supplementary Table 5).

Amygdala reactivity task. In our threat-related amygdala reactivity paradigm, participants complete four blocks of a perceptual face-matching task interleaved with five blocks of a sensorimotor control task. In each face-matching trial, participants view a trio of faces (expressing angry, fearful, surprised or neutral emotions) and select which one of two faces (displayed on the bottom) is identical to the target stimulus (displayed on top). Each block has six trials (balanced for gender) containing stimuli derived from a standard set of facial affect pictures. Blocks are emotion-specific (for example, in the fearful block participants see only faces expressing fear) and block order is pseudo-randomized across participants. Each face trio is displayed for 4 s with a variable interstimulus interval of 2–6 s (mean = 4 s) between presentations, for a total block length of 48 s. In the sensorimotor control task participants view a trio of geometric shapes (circles, horizontal ellipses and vertical ellipses) and select which one of two shapes (displayed on the bottom) is identical to the target shape (displayed on top). Each sensorimotor block consists of six different shape trios that are displayed for 4 s with a fixed interstimulus interval of 2 s between presentations, for a total block length of 36 s. All blocks are preceded by a brief instruction ('Match Shapes' or 'Match Faces') and the total paradigm length is 390 s. Reaction times and accuracy are recorded from an MR-compatible button-box.

Genotyping. Genotyping for 174 participants was conducted by 23andMe (Mountain View, CA, USA). Briefly, genomic DNA from all participants was isolated from buccal cells derived from Oragene DNA self-collection kits (DNA Genotek, Kanata, ON, Canada) customized for 23andMe. DNA extraction and genotyping were performed by the National Genetics Institute (NGI), a CLIA-certified clinical laboratory and subsidiary of Laboratory Corporation of America. The Illumina Omni Express chip and a custom array containing an additional ~300 000 SNPs were used to provide genome-wide data (Tung, Do and Erikkson). Because genotyping for rs1390938 failed on this array, we extracted data for rs6992927, which is in complete LD with rs1390938. An additional 124 participants were directly genotyped for rs1390938 by our team using ABI TaqMan genotyping methods as described above. Of the 298 participants included in the study, 28 were genotyped by both 23andMe and our team; there was 100% genotyping concordance. Genotypes in our sample did not differ significantly from Hardy–Weinberg equilibrium ($P = 0.76$).

BOLD fMRI data acquisition. Participants were scanned using a research-dedicated GE MR750 3T scanner (Piscataway Township, NJ, USA) equipped with high-power high-duty cycle 50-mT/m gradients at 200 T/m/s slew rate, and an eight-channel head coil for parallel imaging at high bandwidth up to 1 MHz at the Duke-UNC Brain Imaging and Analysis Center (Durham, NC, USA). A semiautomated high-order shimming program was used to ensure global field homogeneity. A series of 34 interleaved axial functional slices aligned with the anterior commissure–posterior commissure (AC–PC) plane were acquired for full-brain coverage using an inverse-spiral pulse sequence to reduce susceptibility artifact (TR/TE/FA = 2000 ms/30 ms/60; FOV = 240 mm; 3.75 × 3.75 × 4 mm^3 voxels; interslice skip = 0). Four initial RF excitations were performed (and discarded) to achieve steady-state equilibrium. To allow for spatial registration of each participant's data to a standard coordinate system, high-resolution three-dimensional structural images were acquired in 34 axial slices coplanar with the functional scans (TR/TE/FA = 7.7 s/3.0 ms/12; voxel size = 0.9 × 0.9 × 4 mm^3; FOV = 240 mm, interslice skip = 0).

BOLD fMRI data analysis. The general linear model of SPM8 (http://www.fil.ion.ucl.ac.uk/spm) was used for whole-brain image analysis. Individual subject data were realigned to the first volume in the time series to correct for head motion before being spatially normalized into the standard stereotactic space of the Montreal Neurological Institute template using a 12-parameter affine model. Data were then smoothed to minimize noise and residual differences in individual anatomy with a 6 mm full-width at half-maximum Gaussian filter. Next, the ARtifact detection Tool[43] was used to generate regressors accounting for the possible confounding effects of volumes with large motion deflections (that is, >0.6 mm relative to the previous time frame) or spiking artifacts (that is, global mean intensity 2.5 s.d.'s from the entire time series). Five participants, who had more than 5% of their acquisition volumes flagged by ARtifact detection Tool, were dropped from analyses.

Following preprocessing, linear contrasts employing canonical hemodynamic response functions were used to estimate task-specific (that is, Faces > Shapes) BOLD responses for each individual. Individual contrast images (that is, weighted sum of the beta images) were then used in second-level random effects models accounting for scan-to-scan and participant-to-participant variability to determine mean task-specific regional responses using one-sample *t*-tests. A voxel-level statistical threshold of $P < 0.05$, family-wise error corrected for multiple comparisons across the amygdala ROIs, and a cluster-level extent threshold of 10 contiguous voxels was applied to this analysis. Our bilateral amygdala ROIs were created from the Automated Anatomical Labeling atlas[44] using the Wake Forest University PickAtlas toolbox in SPM8. Because of the potential for signal loss and noise often observed in the amygdala and adjacent regions, single-subject BOLD fMRI data were included in subsequent analyses only if there was a minimum of 90% signal coverage in the amygdala ROIs. Four participants had <90% coverage and were dropped from analyses.

BOLD parameter estimates from the maximal voxels within the right and left amygdala clusters exhibiting main effects of task were extracted using the VOI tool in SPM8 and exported for regression analyses in SPSS (v.18). Extracting parameter estimates from maximal voxels activated by our fMRI paradigm, rather than voxels specifically correlated with our independent variables of interest, precludes the possibility of any correlation coefficient inflation that may result when an explanatory covariate is used to select an ROI. We have used this more conservative analytic strategy in recent studies.[42] Gender, self-reported ethnicity (dummy coded as Caucasian/Not Caucasian, African American/Not African American, Asian/Not Asian, Latino/Not Latino and Other/Not Other), and the presence of an Axis I or Axis II disorder were included as covariates in all analyses.

DNA sequencing

The *VMAT1* (*SLC18A1*) gene is located on chromosome 8, 20 046 660–20 084 906bp (www.genome.ucsc.edu). It consists of 16 exons spanning 38 346 bp that encodes 525 amino acids (NM_003053; www.ncbi.nlm.nih.gov). DNA samples from BPD type I patients, as diagnosed by Diagnostic and Statistical Manual of Mental Disorders, Fourth Edition criteria, were obtained from the NIMH Genetics Initiative on BPD (www.nimhgenetics.org). Sanger sequencing of all *VMAT1* exons was carried out in 196 BPD individuals, except for exons 2 and 3 for which 390 BPD and 196 Caucasian controls were sequenced. The *VMAT1* gene exons and exon–intron boundaries were sequenced using exon-specific primers (Supplementary Table 6). *hVMAT1* custom-DNA-oligomers (Integrated DNA Technologies (IDT), San Jose, CA, USA) were designed for each exon using the Primer Select feature on the IDT website. Primer solutions of 0.1 mM were prepared by adding appropriate amount of dH_2O to the lyophilized primer pellet provided. The primer solutions were diluted 10-fold to prepare working stock solutions used in PCRs. A standard PCR was used to amplify each exonic region separately. Each PCR was comprised of a cocktail of 2.5 μl GeneAmp 10 × buffer containing 15 mM magnesium chloride (ABI, Foster City, CA, USA), 1 μl GeneAmp dNTP mix (ABI), 1 μl each of forward and reverse primers, 0.25 μl of AmpliTaq DNA polymerase (5 U/μl; ABI), 20.25 μl of dH_2O and 1 μl of 10 ng/μl DNA. The PCR was then run according to the following protocol (Supplementary Table 6): 95 °C hold for 5 min, followed by 35 cycles of 95 °C for 30 s, annealing temperature for 30 s and 72 °C for 1 min, and then a 72 °C hold for 7 min followed by a 4 °C hold. The PCR product was verified by gel electrophoresis by running 10 μl of product and 2 μl 6 × loading dye (Sigma-Aldrich, St Louis, MO, USA) on a 2% agarose gel stained with ethidium bromide. DNA bands were visualized using TransUV light waves and were checked for appropriate band size against a ΦX174 DNA/*Hae*III digest marker (Promega, Madison, WI, USA). The PCR products were then prepared for Sanger sequencing by degrading primers and dephosphorylating excess nucleotides using Exo-SapIT (Affymetrix, Santa Clara, CA, USA) as follows: 2 μl Exo-SAPIt was added to 10 μl of PCR product and treated under the following conditions in a thermal cycler (37 °C hold for 20 min and 80 °C hold for 20 min).

Samples were sequenced by big-dye termination chemistry Sanger sequencing at the Nucleic Acid/PCR core (NAPcore) facility at the Joseph Stokes Jr Research Institute (see http://www.research.chop.edu/cores/napcore/index.php for further details). Sequencing reactions were prepared using 10 ng DNA per 100 bp sequence, 2 pM primer (1 μl of 2 μM) and quantity sufficient dH_2O to achieve 18 μl total volume. Sequencing results were analyzed with the Sequencher program (Gene Codes Corporation, Ann Arbor, MI, USA) to detect SNPs. All SNPs found with this program were confirmed through a new PCR and re-sequencing of the sample in which the variant was found.

Genotyping

Genotyping of the functional rare variants Phe84Ser (rs17215801) and Arg138Leu (rs148468662) was performed in BPD patients ($n = 4023$) and normal controls ($n = 3305$) of European descent from the NIMH Genetic Initiative (www.nimhgenetics.org) using standard ABI TaqMan genotyping protocols. For each SNP, a custom TaqMan allelic discrimination assay was designed and ordered using the FileBuilder 3.1 software (ABI, Life Technologies, Grand Island, NY, USA). Quality control was assured by including DNA of probands with rare variants confirmed by sequencing as positive controls. Results were imported into TaqMan Genotyper software for quality control and final analysis. All individuals with a rare variant allele were confirmed by Sanger sequencing. Genotyping of the common variants Thr4Pro (rs2270641), Ser98Thr (rs2270637) and Thr136Ile (rs1390938) in the human imaging data set (see above) was carried out using standard TaqMan genotyping protocols, unless otherwise noted (ABI assays were Thr4Pro: C_22271506_10; Ser98Thr: C_2716008_1_; and Thr136Ile: C_8804621_1_).

In silico analysis

The schematic of VMAT1 protein sequence (Figure5b) was rendered using the TEXtopo package (version 1.4) in the free cross-platform LaTex editor TexMakerX version 2.1 (SVN 1774) for Windows downloaded from http://texmakerx.sourceforge.net. The LaTex program for the rendering (available on request) was compiled within TexMakerX to generate a portable document file (.pdf) that was then imported into Microsoft Powerpoint for labeling of common and rare variant amino acids.

RESULTS

In vitro analyses of common variants

Because of previous associations between Thr136Ile genotype and BPD,[27] as well as both Thr4Pro and Ser98Thr genotypes with SZ,[23–26] we used a translational research approach to investigate potential functional effects of these variants. Full-length human *VMAT1* cDNA is expressed in substantia nigra and was cloned for subsequent experiments (Figure 1a). VMAT1 protein expression in transfected CV-1 cell lines was quantitated by western blot and a pharmacological profile consistent with VMAT1 function was revealed in these transfected cells (Figures 1b and c). We then used site-directed mutagenesis to generate constructs representing all haplotypes common in European populations and measured vesicular monoamine transport in cells transfected transiently with each construct (Figure 1d). The Thr–Ser–Ile haplotype containing 136Ile led to a 13.3-fold increase in NE uptake, a 2.4-fold increase in DA uptake and a 3.7-fold increase in 5-HT uptake as compared with other common haplotypes (Figure 2), which on the other hand were functionally nearly equivalent. Experiments with stably transfected cell lines showed that 136Ile itself is responsible for the increase in transporter capacity, independent of the background haplotype on which it resides (Supplementary Figure 1). This variant was associated previously with BPD,[27] anxiety-related personality traits[29] and cognitive phenotypes in SZ.[28]

Prefrontal function and *VMAT1* Thr136Ile

Given the strong *in vitro* data for an effect of the Thr136Ile variant on monoamine transport, we tested the effects of Thr136Ile in a single region of interest (ROI), the medial PFC, that was previously shown to activate with negative words.[35] For the pooled sample of 85 healthy and 17 major depressive disorder (MDD) subjects, Thr136 homozygotes ($n = 63$) were more responsive to negative words than Ile136 carriers ($n = 39$, including 31 Ile136/Ile136 homozygotes and 8 Thr136/Ile136 heterozygotes) after controlling for sex, age, race and MDD diagnosis ($P = 0.008$, $F_{1,96} = 7.2$; Figure 3a and b). We then tested an additive genetic model using all three genotype groups ($n = 63$, 31 and 8) and found a similar result ($P = 0.01$, $\beta = 0.27$), adjusted for gender, self-reported ethnicity and MDD diagnosis. Finally, we explored responses to negative words voxel-wise throughout the brain. No gene effects survived conservative whole-brain correction ($P > 0.05$, family-wise error correction), but uncorrected effects of Ile136 genotype were apparent in the task-related medial PFC region and adjacent pregenual ACC (Figure 3c). There was no effect of Thr4Pro ($P = 0.38$, $F = 0.78$, d.f. = 1,97) and Ser98Thr ($P = 0.52$, $F = 0.43$, d.f. = 1,97) on medial PFC activation, which converges with previous *in vitro* results. Finally, based on gene effects on threat-related amygdala activation (see below), we also performed an analysis restricted to bilateral amygdala, which showed no effects of Thr136Ile in the word task ($P > 0.05$, family-wise error correction).

Amygdala reactivity and *VMAT1* Thr136Ile

To further explore the effects of the Thr136Ile polymorphism on emotion processing, we examined whether Thr136Ile genotype is associated with individual differences in amygdala reactivity to threat. Genotype and neuroimaging data were available from 298 participants who completed the Duke Neurogenetics Study, an ongoing protocol assessing a wide range of behavioral and biological phenotypes among young adult volunteers. Genotypes were imputed for rs1390938 by using single-nucleotide polymorphism (SNP) rs6992927, which is in complete linkage disequilibrium (LD) for 174 individuals, whereas direct genotyping of rs1390938 was carried out for 124 subjects. Concordance rates for subjects who we genotyped using both methods was 100%. Blood oxygenation level-dependent (BOLD) fMRI revealed robust bilateral amygdala reactivity across all participants (Figure 4a). Regression analyses with gender, self-reported ethnicity and the presence of Axis I or Axis II psychopathology included as

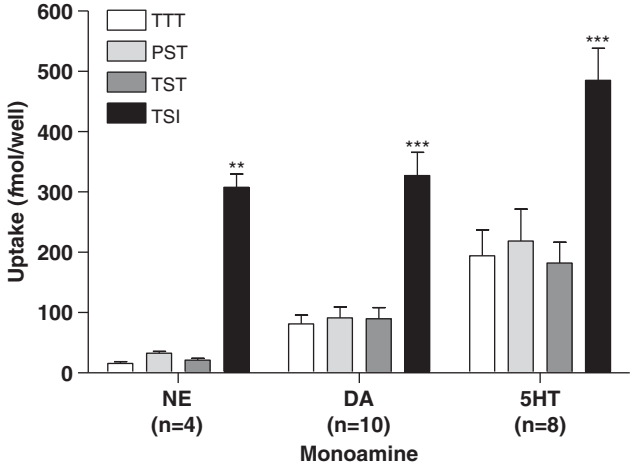

Figure 2. The haplotype containing the common variant Thr136Ile leads to increased monoamine uptake *in vitro*. Common vesicular monoamine transporter 1 (VMAT1) haplotypes were assayed for the uptake of ^{3}H-labeled monoamines (NE, norepinephrine; DA, dopamine; or 5-HT, serotonin). The mean ± s.e.m. for each assayed construct is shown. Analysis of variance (ANOVA) with Tukey's honestly significant difference (HSD) *post hoc* analysis. $^{**}P < 0.01$; $^{***}P < 0.001$.

covariates revealed a significant effect of Thr136Ile genotype on the overall magnitude of threat-related amygdala reactivity (overall model: $F(7,290) = 2.87$, $P = 0.006$, $R^2 = 0.065$; standardized $\beta = 0.13$, $t = 2.25$, $P = 0.025$; change in the overall model after accounting for covariates, $\Delta F(1,290) = 5.08$, $\Delta R^2 = 0.016$). Specifically, Ile136 (that is, A allele) carriers ($n = 121$) had heightened left amygdala reactivity relative to Thr136 (that is, G allele) homozygotes ($n = 177$; Figure 4b). Results were similar if participants were grouped across all three resulting genotypes (Supplementary Figure 2). There was no such genotype effect on overall reactivity of the right amygdala (overall model: $F(7,290) = 2.10$, $P = 0.04$, $R^2 = 0.048$; Thr136Ile standardized $\beta = 0.07$, $t = 1.17$, $P = 0.24$). However, in the right (but not left) amygdala, the number of A alleles was marginally associated with reduced amygdala habituation over time (standardized $\beta = 0.11$, $t = 1.89$, $P = 0.06$; Supplementary Figure 3). Consistent with the *in vitro* and negative word data described above, there were no effects of Thr4Pro ($t = 1.39$, $P = 0.17$) or Ser98Thr ($t = 0.07$ $P = 0.94$) on amygdala reactivity.

Rare variants in *VMAT1* are functional and associated with BPD

Given that the common variant Thr136Ile influences negative emotion processing, we then investigated if rare missense *VMAT1* variants are functional and are associated with BPD, a phenotype characterized by abnormal affect, recurring depression and mania.

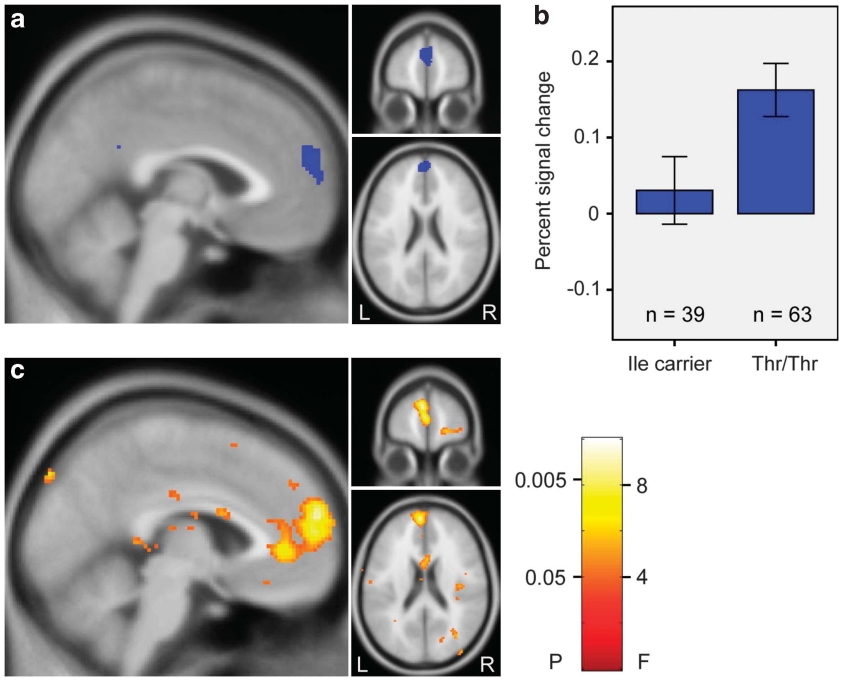

Figure 3. Effect of vesicular monoamine transporter 1 (*VMAT1*) Thr136Ile genotype on medial prefrontal cortex (PFC) responses to negative words. (**a**) Task effect (negative–neutral word contrast) in the medial PFC for healthy participants is shown in three sections: sagittal at $x = -2$ (left), coronal at $y = 56$ (upper right) and horizontal at $z = 22$ (lower right). Blue area indicates uncorrected two-sided $P < 0.001$. L, left; R, right. This cluster was extracted as a region of interest to test for the effect of VMAT1 genotype. (**b**) Effect of VMAT1 genotype on percent signal change in the medial PFC region of interest shown in (**a**) ($P = 0.008$). Error bars indicate s.e.m. (**c**) Exploratory analysis of gene effects elsewhere in the brain. Effect of VMAT1 genotype (Thr homozygotes vs Ile carriers) is shown in three sections: sagittal at $x = -4$ (left), coronal at $y = 58$ (upper right) and horizontal at $z = 20$ (lower right). Scale bar represents uncorrected *P*-value and F-statistic.

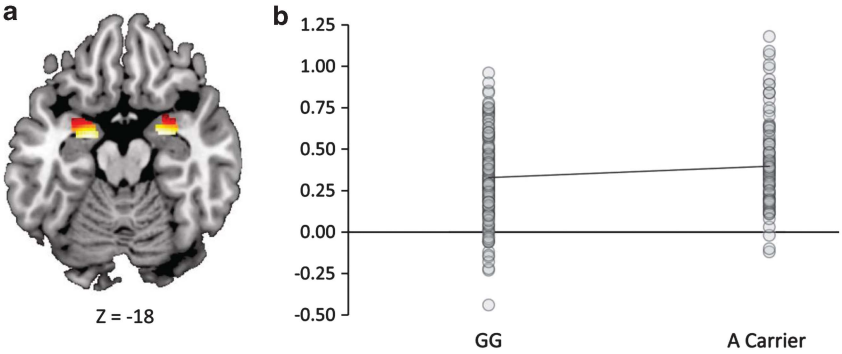

Figure 4. Genetic variation in human vesicular monoamine transporter 1 (*VMAT1*) is associated with threat-related amygdala reactivity. (**a**) Bilateral threat-related amygdala reactivity across all participants. Right hemisphere: Montreal Neurological Institute (MNI) coordinates = 28, −4 and −20 ($t = 25.59$, $P < 0.01$), cluster size = 218 voxels. Left hemisphere: MNI coordinates = −22, −6 and −18 ($t = 24.80$, $P < 01$), cluster size = 170 voxels. (**b**) An allele carrier (136Ile) ($n = 121$) had increased the left amygdala reactivity relative to G homozygotes (136Thr) ($n = 177$).

Sequencing

DNA Sanger sequencing of BPD patients identified several novel and rare variants (Supplementary Table 1). Interestingly, we found the majority of rare and novel variants in the 5′ region of the gene, particularly in exons 2 and 3 that code for the first intravesicular loop (Figure 5a and b). Comparison of amino-acid sequences from different species indicates strong conservation at positions of common and rare variants (Figure 5b). Comparison of sequencing results of rare variants in BPD individuals with normal controls from the 1000 Genome project shows that the global burden of rare variants was increased in the BPD group (Supplementary Table 2). Interestingly, several novel variants were only detected in the BPD group but were absent in the controls (Supplementary Table 1).

In vitro analyses of rare variants

To investigate whether the rare missense variants have a functional effect on protein transporter function, we assessed monoamine uptake *in vitro* for Gln10Arg, Phe84Ser, Ala101Pro, Arg138Leu and Leu392Val. Phe84Ser robustly increased monoamine uptake in particular for DA (Figure 6) and the three variants, Ala101Pro, Arg138Leu and Leu392Val decreased uptake, with Arg138Leu showing the largest effect for DA, although similar results were also obtained for 5-HT and NE (Figure 6 and Supplementary Figure. 4).

Genotyping of rare variants

Because of the robust functional effects of Phe84Ser and Arg138Leu, we genotyped these rare variants in a large sample of BPD cases ($n = 4023$) and controls ($n = 3305$) of European descent using standard ABI TaqMan 'assays by design'. DNA samples were obtained from the National Institute of Mental Health (NIMH) genetics initiative. The Ser84 allele was absent in controls but present in seven BPD individuals, including one homozygote and six heterozygotes (Table 1; Fisher exact test, $P = 0.009$). The Leu138 frequency did not differ statistically between cases and controls (Table 1). Haplotype analysis of the individuals with the rare variant Phe84Ser showed that all subjects

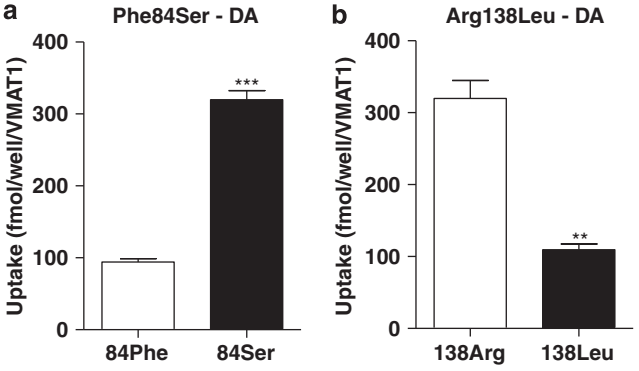

Figure 6. The rare vesicular monoamine transporter 1 (*VMAT1*) variant Phe84Ser and Arg138Leu lead to increased and decreased dopamine (DA) uptake *in vitro*, respectively. (**a**) Phe84Ser DA uptake *in vitro*. (**b**) Arg138Leu DA uptake *in vitro*. Data are expressed as the mean ± s.e.m. The Student's *t*-test was used to compare monoamine uptake for rare variants. $^{**}P < 0.01$ and $^{***}P < 0.001$.

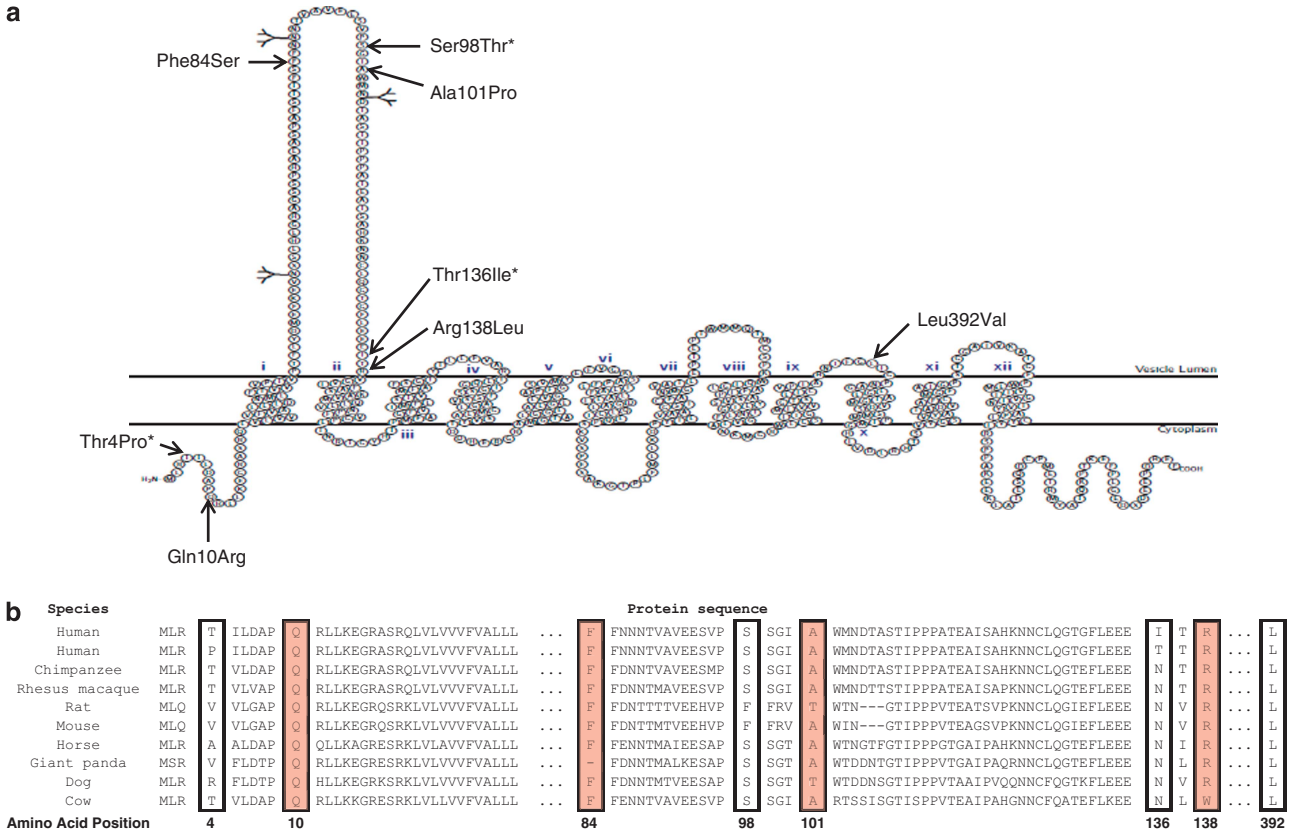

Figure 5. Common and rare vesicular monoamine transporter 1 (*VMAT1*) variants detected by sequencing. (**a**) Predicted topology of full-length human VMAT1 protein showing 12 transmembrane domains and clustering of variation in the first intravesicular loop; *indicates common variant minor allele frequencies (MAF) > 20%. (**b**) Comparison of amino-acid sequences from different species indicates strong conservation at positions of common and rare variants. Rare variants are highlighted in red.

Table 1. Case–control study of rare functional non-synonymous SNPs in *VMAT1*

	Bipolar	*Controls*	P-*value*
F84S			
Phe84 allele	7846	6610	0.009
Ser84 allele	8	0	
R138L			
Arg138 allele	8039	6586	0.199
Leu138 allele	7	2	

Abbreviations: NIMH, National Institute of Mental Health; SNP, single-nucleotide polymorphism; VMAT1, vesicular monoamine transporter 1. The functional amino-acid polymorphisms Phe84Ser and Arg138Leu were genotyped in 4023 BPD cases and 3305 controls of European descent using standard ABI Taqman 'assay by design' genotyping methods. DNA samples were obtained from the NIMH genetics initiative. Results show that the Ser84 allele was absent in controls but present in seven BPD individuals, one homozygote and six heterozygotes (Fisher'a exact test). The Arg138Leu variant frequency did not differ statistically significant between cases and controls.

had almost exclusively the same halplotype Thr–Ser–Thr, indicative of a common origin and founder population effect[45] (Supplementary Table 3).

DISCUSSION

This study was undertaken to determine functional effects of common *VMAT1* variants on monoamine signaling, emotional brain circuitry and risk for psychopathology. In addition, we investigated the functional consequences of rare variants identified through deep sequencing in patients with BPD. For several decades, it has been well-recognized that differences in monoamine neurotransmission contribute to variance in normal behavior, emotionality and psychopathology. In part, this variation is driven by genetic factors, yet little is known about the identity and neurobiological role of polymorphisms that contribute to this variance. Although progress has been made in disentangling these complex phenomena, mostly through imaging genetics approaches that focus on plasma membrane transporters and post-synaptic receptors,[3] relatively little is known about presynaptic mechanisms. Such presynaptic components are likely critical as they are a principal common entry point for monoamine homeostasis and may represent a shared pathway for vulnerability to a range of neuropsychiatric phenotypes.

Here, we show that the 136Ile allele of a common *VMAT1* genetic polymorphism (rs1390938) leads to increased monoamine transport *in vitro*. To further investigate the functional effects of this 'hyperfunction' allele on emotional brain circuitry, we utilized two imaging genetics data sets. In one study, we found that carriers of the *VMAT1* 'hyperfunction' allele showed diminished hemodynamic responses to negative emotional words in the medial PFC and pregenual ACC when compared with Thr136 homozygotes ($P = 0.008$, $F_{1,96} = 7.2$; Figure 3a and b). These data suggest that the *VMAT1* 'hyperfunction' allele may predispose certain individuals to a diminished cortical response to negative stimuli. Activity of these prefrontal regions is a critical component of regulating emotional arousal, particularly those triggered by the amygdala in response to environmental stimuli.

In the second imaging genetics study, we examined the effects of rs1390938 on threat-related amygdala reactivity directly. Our results show that the *VMAT1* 'hyperfunction' allele was associated with increased amygdala reactivity (Figure 4) and decreased habituation. These patterns are consistent with a number of mood and anxiety disorders, including increased reactivity in BPD during mania[46] and diminished habituation in post-traumatic stress disorder.[47] Notably, these disorders have also been associated with diminished prefrontal activation as was found with the 'hyperfunction' allele in our other imaging genetics study. The laterality of *VMAT1* effects on amygdala reactivity (left hemisphere) and habituation (right hemisphere) may reflect the relative contribution of the left and right amygdala to sustained evaluation versus phasic responsiveness to stimuli, respectively.[48]

The divergent effects of the 'hyperfunction' allele on prefrontal (relatively decreased) and amygdala (relatively increased) suggest that common variation in *VMAT1* can have region- and task-specific effects.[49,50] Importantly, these divergent cortical and subcortical effects are consistent with those previously reported for other common polymorphisms, resulting in relatively increased monoamine signaling.[51,52] Moreover, these divergent effects are consistent with patterns of dysfunction in mood and anxiety disorders characterized by increased amygdala reactivity and decreased prefrontal activity.[53] Thus, the results of our imaging genetic studies suggest that the 136Ile allele is associated with a pattern of dysfunctional prefrontal and amygdala function that may predispose carriers to the development of mood and anxiety disorders. Studies are now needed to evaluate directly the impact of the 136Ile allele on corticolimbic circuit function in mood and anxiety disorders, as well as on the structural and functional connectivity of this circuit during explicit emotion regulation and fear learning tasks, which directly engage this circuitry.

It should be noted that the majority of subjects in our two imaging genetics studies were healthy individuals; however, impaired social cognition and emotion processing are hallmarks of several psychiatric disorders such as SZ and BPD.[54,55] In fact, the Thr136Ile variant was recently shown to be associated with several cognitive phenotypes in SZ[28] and anxiety-related personality traits.[29] Other SNPs that are in LD with Thr136Ile (rs1390938) have been associated with major depression[56] and anorexia nervosa.[57] The association of the functional Thr136Ile SNP with several other psychiatric phenotypes suggests that this *VMAT1* variant might influence brain circuits involved in emotion processing, which are shared by several psychiatric disorders but not disease *per se*. In line with this hypothesis is the observation that although the Thr136Ile polymorphism was previously shown to be associated with BPD,[27] with the 136Ile being more common in the control population, subsequent genome-wide association studies failed to establish a strong relationship between rs1390938 and disease. This lack of replication could be due to the complex mode of inheritance, complex LD structure resulting in imperfect r^2-diluting signal detection and/or clinical heterogeneity. Extensive subphenotyping including endophenotypic measures as well as subanalyses of patients with linkage signals to chromosome 8p might strengthen the power to detect an effect of Thr136Ile on disease risk in future studies.[58,59]

Although genome-wide association studies failed to identify *VMAT1* as a major susceptibility gene for BPD, owing to the above-mentioned reasons, we conducted deep sequencing to identify rare variants possibly associated with disease. Sequencing detected several rare missense variants in BPD patients (Figure 5). Interestingly, most of these novel rare variants are located in the first intravesicular loop of *VMAT1*, a region that has been implicated in regulating transport of neurotransmitter into vesicles.[11] In fact, our *in vitro* analyses of the rare variant Ser84 and the common allele Ile136 show that these alleles lead to increased vesicle filling (Figure 2, Figure 6 and Supplementary Figure 1), whereas the rare Leu138 variant leads to decreased vesicle filling of monoamines (Figure 6). Association analyses of the rare variants Phe84Ser and Arg138Leu in 4023 BPD patients and 3305 controls show that the Ser84 allele was only present in BPD individuals but absent in controls (Table 1). Given that Thr136Ile leads to increased monoamine transport and has an effect on interindividual responses to medial PFC activation of negative words and

threat-related amygdala reactivity, the rare Phe84Ser variant may have similar effect on these brain circuits. Owing to the low prevalence of the Ser84 allele, imaging genetic studies are not feasible at this point. Although it is unknown how large such an effect of this rare *VMAT1* variant will be in individuals with BPD, we speculate that rare variants might have larger effects on function. Future studies are needed to comprehensively investigate SNP-dosage effects on transporter function *in vivo*.

In summary, we show that the common Thr136Ile and rare Phe84Ser variant are located in close proximity to a regulatory region within the *VMAT1* gene and lead to hyperfunction of vesicular transport *in vitro*. Thr136Ile (rs1390938) has an effect on interindividual responses to emotion processing *in vivo* in two separate fMRI paradigms, providing insight into a mechanism for how genetic variation in presynaptic vesicular transport of monoamines can influence emotionality. Although emotion responding is critical for normal adaptive behavior, it is clear that interindividual variance exists, with extremes often observed in psychopathology. Our study provides convergent neurobiological evidence for a role of both rare and common *VMAT1* variants in neural emotion processing and related psychopathology and advances our understanding of the complex mechanisms regulating monoaminergic signaling and emotional behavior.

CONFLICT OF INTEREST

Dr Lohoff declares that he is named as one of the inventors of a patent involving human genetic *VMAT1* variants (US Patent No. 7 736 852). Within the 3-year period before submission of the manuscript, Dr Mickey has received salary support from St Jude Medical for research unrelated to this manuscript, and Dr Zubieta has served as a paid consultant for Eli Lilly, Johnson & Johnson, Merck and Abbott for work unrelated to this manuscript. All remaining authors declare no conflict of interest.

ACKNOWLEDGEMENTS

This work was supported by the Center for Neurobiology and Behavior, Department of Psychiatry, University of Pennsylvania. Financial support is gratefully acknowledged from National Institutes of Health Grants (NIH K08MH080372 to FWL), NCRR (UL1 RR 024986), NIMH (P01 MH 42251, R25 MH 6374 and K23 MH 074459), NIDA (R01 DA 016423 and R01 DA 022520, and 026222 and 031579) and the Phil F Jenkins Research Fund.

REFERENCES

1 Dalgleish T. The emotional brain. *Nat Rev Neurosci* 2004; **5**: 583–589.
2 Bouchard Jr TJ, McGue M. Genetic and environmental influences on human psychological differences. *J Neurobiol* 2003; **54**: 4–45.
3 Bevilacqua L, Goldman D. Genetics of emotion. *Trends Cogn Sci* 2011; **15**: 401–408.
4 Liu Y, Peter D, Roghani A, Schuldiner S, Privé GG, Eisenberg D *et al.* A cDNA that suppresses MPP+ toxicity encodes a vesicular amine transporter. *Cell* 1992; **70**: 539–551.
5 Peter D, Finn JP, Klisak I, Liu Y, Kojis T, Heinzmann C *et al.* Chromosomal localization of the human vesicular amine transporter genes. *Genomics* 1993; **18**: 720–723.
6 Erickson JD, Schafer MK, Bonner TI, Eiden LE, Weihe E. Distinct pharmacological properties and distribution in neurons and endocrine cells of two isoforms of the human vesicular monoamine transporter. *Proc Natl Acad Sci USA* 1996; **93**: 5166–5171.
7 Peter D, Liu Y, Sternini C, de Giorgio R, Brecha N, Edwards RH. Differential expression of two vesicular monoamine transporters. *J Neurosci* 1995; **15**: 6179–6188.
8 Ibanez-Sandoval O, Tecuapetla F, Unal B, Shah F, Koós T, Tepper JM. Electrophysiological and morphological characteristics and synaptic connectivity of tyrosine hydroxylase-expressing neurons in adult mouse striatum. *J Neurosci* 2010; **30**: 6999–7016.
9 Ashe KM, Chiu WL, Khalifa AM, Nicolas AN, Brown BL, De Martino RR *et al.* Vesicular monoamine transporter-1 (VMAT-1) mRNA and immunoreactive proteins in mouse brain. *Neuro Endocrinol Lett* 2011; **32**: 253–258.
10 Hansson SR, Hoffman BJ, Mezey E. Ontogeny of vesicular monoamine transporter mRNAs *VMAT1* and VMAT2. I. The developing rat central nervous system. *Brain Res Dev Brain Res* 1998; **110**: 135–158.
11 Brunk I, Blex C, Rachakonda S, Höltje M, Winter S, Pahner I *et al.* The first luminal domain of vesicular monoamine transporters mediates G-protein-dependent regulation of transmitter uptake. *J Biol Chem* 2006; **281**: 33373–33385.
12 Schildkraut JJ, Kety SS. Biogenic amines and emotion. *Science (New York, NY)* 1967; **156**: 21–37.
13 Goodwin FK, Bunney Jr WE. Depressions following reserpine: a reevaluation. *Semin Psychiatry* 1971; **3**: 435–448.
14 Bant WP. Antihypertensive drugs and depression: a reappraisal. *Psychol Med* 1978; **8**: 275–283.
15 Widmer RB. Reserpine: the maligned antihypertensive drug. *J Fam Pract* 1985; **20**: 81–83.
16 Wang YM, Gainetdinov RR, Fumagalli F, Xu F, Jones SR, Bock CB *et al.* Knockout of the vesicular monoamine transporter 2 gene results in neonatal death and supersensitivity to cocaine and amphetamine. *Neuron* 1997; **19**: 1285–1296.
17 Takahashi N, Miner LL, Sora I, Ujike H, Revay RS, Kostic V *et al.* VMAT2 knockout mice: heterozygotes display reduced amphetamine-conditioned reward, enhanced amphetamine locomotion, and enhanced MPTP toxicity. *Proc Natl Acad Sci USA* 1997; **94**: 9938–9943.
18 Fon EA, Pothos EN, Sun BC, Killeen N, Sulzer D, Edwards RH. Vesicular transport regulates monoamine storage and release but is not essential for amphetamine action. *Neuron* 1997; **19**: 1271–1283.
19 Fumagalli F, Gainetdinov RR, Wang YM, Valenzano KJ, Miller GW, Caron MG. Increased methamphetamine neurotoxicity in heterozygous vesicular monoamine transporter 2 knock-out mice. *J Neurosci* 1999; **19**: 2424–2431.
20 Narboux-Neme N, Sagné C, Doly S, Diaz SL, Martin CB, Angenard G *et al.* Severe serotonin depletion after conditional deletion of the vesicular monoamine transporter 2 gene in serotonin neurons: neural and behavioral consequences. *Neuropsychopharmacology* 2011; **36**: 2538–2550.
21 Taylor TN, Caudle WM, Miller GW. VMAT2-Deficient mice display nigral and extranigral pathology and motor and nonmotor symptoms of Parkinson's disease. *Parkinson's Disease* 2011; **2011**.
22 Fukui M, Rodriguiz RM, Zhou J, Jiang SX, Phillips LE, Caron MG *et al.* Vmat2 heterozygous mutant mice display a depressive-like phenotype. *J Neurosci* 2007; **27**: 10520–10529.
23 Richards M, Iijima Y, Kondo H, Shizuno T, Hori H, Arima K *et al.* Association study of the vesicular monoamine transporter 1 (*VMAT1*) gene with schizophrenia in a Japanese population. *Behav Brain Funct* 2006; **2**: 39.
24 Bly M. Mutation in the vesicular monoamine gene, SLC18A1, associated with schizophrenia. *Schizophr Res* 2005; **78**: 337–338.
25 Chen SF, Chen CH, Chen JY, Wang YC, Lai IC, Liou YJ *et al.* Support for association of the A277C single nucleotide polymorphism in human vesicular monoamine transporter 1 gene with schizophrenia. *Schizophr Res* 2007; **90**: 363–365.
26 Lohoff FW, Weller AE, Bloch PJ, Buono RJ, Doyle GA, Ferraro TN *et al.* Association between polymorphisms in the vesicular monoamine transporter 1 gene (*VMAT1*/SLC18A1) on chromosome 8p and schizophrenia. *Neuropsychobiology* 2008; **57**: 55–60.
27 Lohoff FW, Dahl JP, Ferraro TN, Arnold SE, Gallinat J, Sander T *et al.* Variations in the vesicular monoamine transporter 1 gene (*VMAT1*/SLC18A1) are associated with bipolar I disorder. *Neuropsychopharmacology* 2006; **31**: 2739–2747.
28 Need AC, Keefe RS, Ge D, Grossman I, Dickson S, McEvoy JP *et al.* Pharmacogenetics of antipsychotic response in the CATIE trial: a candidate gene analysis. *Eur J Hum Genet* 2009; **17**: 946–957.
29 Lohoff FW, Lautenschlager M, Mohr J, Ferraro TN, Sander T, Gallinat J *et al.* Association between variation in the vesicular monoamine transporter 1 gene on chromosome 8p and anxiety-related personality traits. *Neurosci Lett* 2008; **434**: 41–45.
30 Green EK, Grozeva D, Jones I, Jones L, Kirov G, Caesar S *et al.* The bipolar disorder risk allele at CACNA1C also confers risk of recurrent major depression and of schizophrenia. *Mol Psychiatry* 2010; **15**: 1016–1022.
31 Craddock N, O'Donovan MC, Owen MJ. Genes for schizophrenia and bipolar disorder? Implications for psychiatric nosology. *Schizophr Bull* 2005; **32**: 9–16.
32 Craddock N, Owen MJ. The Kraepelinian dichotomy—going, going. but still not gone. *Br J Psychiatry* 2010; **196**: 92–95.
33 Erickson JD, Eiden LE, Hoffman BJ. Expression cloning of a reserpine-sensitive vesicular monoamine transporter. *Proc Natl Acad Sci USA* 1992; **89**: 10993–10997.
34 Essand M, Vikman S, Grawé J, Gedda L, Hellberg C, Oberg K *et al.* Identification and characterization of a novel splicing variant of vesicular monoamine transporter 1. *J Mol Endocrinol* 2005; **35**: 489–501.
35 Mickey BJ, Zhou Z, Heitzeg MM, Heinz E, Hodgkinson CA, Hsu DT *et al.* Emotion processing, major depression, and functional genetic variation of neuropeptide Y. *Arch Gen Psychiatry* 2011; **68**: 158–166.
36 Hsu DT, Langenecker SA, Kennedy SE, Zubieta JK, Heitzeg MM. fMRI BOLD responses to negative stimuli in the prefrontal cortex are dependent on levels of recent negative life stress in major depressive disorder. *Psychiat Res* 2010; **183**: 202–208.
37 Heitzeg MM, Nigg JT, Yau WY, Zubieta JK, Zucker RA. Affective circuitry and risk for alcoholism in late adolescence: differences in frontostriatal responses between vulnerable and resilient children of alcoholic parents. *Alcohol Clin Exp Res* 2008; **32**: 414–426.

38 Bradley MM, Lang PJ. *Affective Norms for English Words (ANEW): Stimuli, Instruction Manual and Affective Ratings*. The Center for Research in Psychophysiology, University of Florida: Gainesville, FL, 1999.
39 Kraemer HC, Thiemann S. *How Many Subjects? Statistical Power Analysis in Research*. Sage Publications: Newbury Park, 1987.
40 Lancaster JL, Woldorff MG, Parsons LM, Liotti M, Freitas CS, Rainey L *et al.* Automated Talairach atlas labels for functional brain mapping. *Hum Brain Mapp* 2000; **10**: 120–131.
41 Maldjian JA, Laurienti PJ, Kraft RA, Burdette JH. An automated method for neuroanatomic and cytoarchitectonic atlas-based interrogation of fMRI data sets. *NeuroImage* 2003; **19**: 1233–1239.
42 Bogdan R, Hyde LW, Hariri AR. A neurogenetics approach to understanding individual differences in brain, behavior, and risk for psychopathology. *Mol Psychiatry* advance online publication, 22 May 2012; doi:10.1038/mp.2012.35 (e-pub ahead of print).
43 Whitfield-Gabrieli S, Thermenos HW, Milanovic S, Tsuang MT, Faraone SV, McCarley RW *et al.* Hyperactivity and hyperconnectivity of the default network in schizophrenia and in first-degree relatives of persons with schizophrenia. *Proc Natl Acad Sci USA* 2009; **106**: 1279–1284.
44 Tzourio-Mazoyer N, Landeau B, Papathanassiou D, Crivello F, Etard O, Delcroix N *et al.* Automated anatomical labeling of activations in SPM using a macroscopic anatomical parcellation of the MNI MRI single-subject brain. *NeuroImage* 2002; **15**: 273–289.
45 Bevilacqua L, Doly S, Kaprio J, Yuan Q, Tikkanen R, Paunio T *et al.* A population-specific HTR2B stop codon predisposes to severe impulsivity. *Nature* 2010; **468**: 1061–1066.
46 Altshuler L, Bookheimer S, Proenza MA, Townsend J, Sabb F, Firestine A *et al.* Increased amygdala activation during mania: a functional magnetic resonance imaging study. *Am J Psychiatry* 2005; **162**: 1211–1213.
47 Milad MR, Pitman RK, Ellis CB, Gold AL, Shin LM, Lasko NB *et al.* Neurobiological basis of failure to recall extinction memory in posttraumatic stress disorder. *Biol Psychiatry* 2009; **66**: 1075–1082.
48 Costafreda SG, Brammer MJ, David AS, Fu CH. Predictors of amygdala activation during the processing of emotional stimuli: a meta-analysis of 385 PET and fMRI studies. *Brain Res Rev* 2008; **58**: 57–70.
49 Kim MJ, Gee DG, Loucks RA, Davis FC, Whalen PJ. Anxiety dissociates dorsal and ventral medial prefrontal cortex functional connectivity with the amygdala at rest. *Cereb Cortex* 2011; **21**: 1667–1673.
50 Likhtik E, Pelletier JG, Paz R, Pare D. Prefrontal control of the amygdala. *J Neurosci* 2005; **25**: 7429–7437.
51 Caspi A, Hariri AR, Holmes A, Uher R, Moffitt TE. Genetic sensitivity to the environment: the case of the serotonin transporter gene and its implications for studying complex diseases and traits. *Am J Psychiatry* 2010; **167**: 509–527.
52 Buckholtz JW, Callicott JH, Kolachana B, Hariri AR, Goldberg TE, Genderson M *et al.* Genetic variation in MAOA modulates ventromedial prefrontal circuitry mediating individual differences in human personality. *Mol Psychiatry* 2008; **13**: 313–324.
53 Lawrence NS, Williams AM, Surguladze S, Giampietro V, Brammer MJ, Andrew C *et al.* Subcortical and ventral prefrontal cortical neural responses to facial expressions distinguish patients with bipolar disorder and major depression. *Biol Psychiatry* 2004; **55**: 578–587.
54 Bora E, Yucel M, Pantelis C. Cognitive impairment in schizophrenia and affective psychoses: implications for DSM-V criteria and beyond. *Schizophr Bull* 2010; **36**: 36–42.
55 Jabben N, Arts B, van Os J, Krabbendam L. Neurocognitive functioning as intermediary phenotype and predictor of psychosocial functioning across the psychosis continuum: studies in schizophrenia and bipolar disorder. *J Clin Psychiatry* 2010; **71**: 764–774.
56 Shyn SI, Shi J, Kraft JB, Potash JB, Knowles JA, Weissman MM *et al.* Novel loci for major depression identified by genome-wide association study of sequenced treatment alternatives to relieve depression and meta-analysis of three studies. *Mol Psychiatry* 2009; **16**: 202–215.
57 Pinheiro AP, Bulik CM, Thornton LM, Sullivan PF, Root TL, Bloss CS *et al.* Association study of 182 candidate genes in anorexia nervosa. *Am J Med Genet B Neuropsychiatr Genet* 2010; **153B**: 1070–1080.
58 Braff DL, Greenwood TA, Swerdlow NR, Light GA, Schork NJ. Advances in endophenotyping schizophrenia. *World Psychiatry* 2008; **7**: 11–18.
59 Gottesman II, Gould TD. The endophenotype concept in psychiatry: etymology and strategic intentions. *Am J Psychiatry* 2003; **160**: 636–645.

Supplementary Information accompanies the paper on the Molecular Psychiatry website (http://www.nature.com/mp)